J. Cent. South Univ. (2013) 20: 2314−2322
DOI: 10.1007/s11771-013-1739-9

Springer

Limit analysis of roof collapse in tunnels under seepage forces condition with three-dimensional failure mechanism

QIN Chang-bing(覃长兵), SUN Zhi-bin(孙志彬), LIANG Qiao(梁桥)

School of Civil Engineering, Central South University, Changsha 410075, China

Abstract: The state of roof collapse in tunnels is actually three-dimensional, so constructing a three-dimensional failure collapse mechanism is crucial so as to reflect the realistic collapsing scopes more reasonably. According to Hoek-Brown failure criterion and the upper bound theorem of limit analysis, the solution for describing the shape of roof collapse in circular or rectangular tunnels subjected to seepage forces is derived by virtue of variational calculation. The seepage forces calculated from the gradient of excess pore pressure distribution are taken as external loading in the limit analysis, and it is of great convenience to compute the pore pressure with pore pressure coefficient. Consequently, the effect of seepage forces is taken as a work rate of external force and incorporated into the upper bound limit analysis. The numerical results of collapse dimensions with different rock parameters show great validity and agreement by comparing with the results of that with two-dimensional failure mechanism.

Key words: tunnel; Hoek-Brown criterion; three-dimensional collapse mechanism; seepage force

1 Introduction

Limit analysis method is widely used in geotechnical engineering using linear failure criterion [1−3]. However, a substantial amount of experimental evidence suggested that failure criteria of geotechnical materials were not linear in the stress space, particularly in the range of small normal stress [4−5]. When applying limit analysis method to estimate the influences of a nonlinear failure criterion, the main problem, which many researchers encountered, was how to calculate the rate of work done by external forces and the rate of energy dissipation along velocity discontinuities. YANG et al [6−9] proposed generalized tangential technique, instead of the actual nonlinear failure criterion, to formulate the work and energy dissipation. The advantage of new method could avoid the difficulty of the calculation of external work rate and energy dissipation rate along velocity discontinuities. Employing the nonlinear failure criterion, the potential roof collapse in tunnel is a practical but complicated problem in geotechnical engineering, especially for those with actual failure mechanism. As the actual failure form was three-dimensional and the plane collapse mechanism can just reflect two dimensions in failure surface which is just the imperfection of this method, more and more scholars are committed to exploring three-dimensional analytical method which can satisfy the practical condition well. LAM and FREDLUND [10] extended the slope model with two dimensions to three-dimensional pattern in the method of limit equilibrium, and the three-dimensional FEM was applied to investigate the cylinder stress function of the model. The method can not only simplify the process of data input but also accelerate the speed of calculating the slope safety coefficient, and the results obtained in this way were more accurate by comparing with that in traditional two-dimensional model. Based on the presented two-dimensional failure mechanism, CHEN et al [11] suggested a three-dimensional limit analysis method to calculate the upper bound solution of the safety coefficient for slope. The results remain the advantages of upper bound method when the three-dimensional failure mechanism was employed in the limit analysis. According to the plane analytical method proposed by DONALD and CHEN [12], the slope minimal safety coefficient was derived by constructing a three-dimensional failure mechanism to calculate the rate of external work and the energy dissipation rate.

Owing to the advantages of three-dimensional method over plane analytic way, some scholars set about to employ three-dimensional method to research the stability problem of tunnels. In early study, ANAGNOSTOU and KOVÁRI [13] constructed a three-dimensional failure mechanism in the excavation face of

Foundation item: Project(2013CB036004) supported by the National Basic Research Program of China; Project(51178468) supported by the National Natural Science Foundation of China; Project(2013zzts235) supported by Innovation Fund of Central South University of China
Received date: 2012−09−10; **Accepted date:** 2013−04−10
Corresponding author: QIN Chang-bing; Tel: +86−13549683494; E-mail: chaoyanglaizhe@126.com

earth-pressure-balanced shield tunnel and the stability of excavation face under drainage condition with the method of limit equilibrium was investigated. Meanwhile, the typical three-dimensional conical-shaped failure mechanism in the excavation face of shallow tunnel was proposed by LECA and DORMIEUX [14], which can describe the collapse pattern commendably and precise upper bound solution of supporting pressure in the excavation face of shallow tunnels can be work out. Then SOUBRA et al [15] optimized the conical-shaped failure mechanism of LECA and DORMIEUX [14]. That was to say, the optimized failure mechanism was composed of a series of cones instead of a single cone, which can obtain more optimized upper bound solution of supporting pressure. CHAMBON and CORTÉ [16] applied the centrifugal model test to verify the result of supporting pressure derived through three-dimensional collapse mechanism in the excavation face of shallow tunnels. The result shows that it was in accord with the experimental value and it was more accurate than that with plane failure mechanism [17−20]. MOLLON et al [21] obtained more exact solutions comparing with original upper bound results with the help of spatial discretization technology by point-to-point method to create a three-dimensional failure mechanism.

At present, FRALDI and GUARRACINO [22−23] obtained the analytic solutions for charactering the shape of roof collapse with a plane curved failure mechanism based on upper bound theorem and variational calculation. YANG et al [24−26] derived the exact solution of roof collapse by virtue of constructing a new collapse mechanism for shallow tunnels that the velocity discontinuity curve was extended from the roof of tunnel to ground surface. The three-dimensional stability analysis was primarily used to the tunnel excavation face in shallow tunnel, and nearly no literature was found to study the stability of roof collapse together with three-dimensional failure mechanism. Recently, YANG and HUANG [19] suggested the three-dimensional mechanism to investigate the roof collapse in rectangular tunnel and the analytic solution was derived based on Hoek-Brown failure criterion.

Gradually, water as well as other fluid has a significant influence on the stability of underground structure, thus the effect of water is not ignorable when analyzing the state of tunnels, and some measures or other disposal method should be taken in time so as to guarantee the tunnels or other ground structures are under a safe state. In previous study, LEE and NAM [27] employed the numerical way to study the seepage forces exerting on the structures of tunnel, and then the limit analysis method was adopted to study the stability effect of seepage forces. Employing the nonlinear Hoek-Brown failure criterion [28], YANG [29−30] have obtained the numerical solutions using equivalent Mohr-Coulomb strength parameters. SAADA et al [31] applied limit analysis method to research the slope stability, from which the seepage forces can be calculated from the gradient of excess pore pressure distribution and taken as external loading incorporated to the upper bound limit analysis. In their study, the pore pressure was worked out with pore pressure coefficient method and FE analysis way separately, and it was noticed that the former was very convenient while the latter was more accurate.

2 Three-dimensional rotational failure mode

Certainly, constructing admissible collapse mechanism is the crucial factor in the upper bound theorem of limit analysis. Combining with the actual mechanical characteristics of rock mass over the roof of shallow-buried tunnels, firstly, an arched detaching curve is supposed to describe the two-dimensional shape of roof collapse in *XOZ* coordinate plane, $f(x)$, which extends from rectangular or circular tunnel roof to the ground surface and the two-dimensional collapse surface is generated. Then, for the purpose of obtaining the three-dimensional collapse velocity field, the simplest way is making the curve $f(x)$ rotate 360 °with respect to *Z*-axis based on rotational mechanism. Gradually, the profiles of tunnels can be designed as arbitrary forms, $g(x)$, as shown in Fig. 1.

However, the circular and rectangular shape were adopted in this work so as to simplify the calculation process. Indeed, the circular profile is often chosen in the design of the running tunnel, and the rectangular cross-section is selected to subway station. When the cross-section of tunnel is circular, it remains great difficulty to derive the precise volume and lateral area of the rotational body, so trying to make some simplification is in desperate need. A sphere structure is adopted to simulate the actual circular arch for circle tunnel in the paper. Due to the presence of velocity discontinuity surface, it will induce the plastic flow. Thus, according to Hoek-Brown failure criterion and associated flow rule, the energy dissipation rate along the detaching surface can be computed consequently. Then, by equating the energy dissipation rate to the rate of external work, the virtual work equation which satisfies the velocity boundary condition can be obtained. Meanwhile, in order to get the exact or approximate shape of the collapsing block under a limit state, the variational calculation should be used to minimize the objective function.

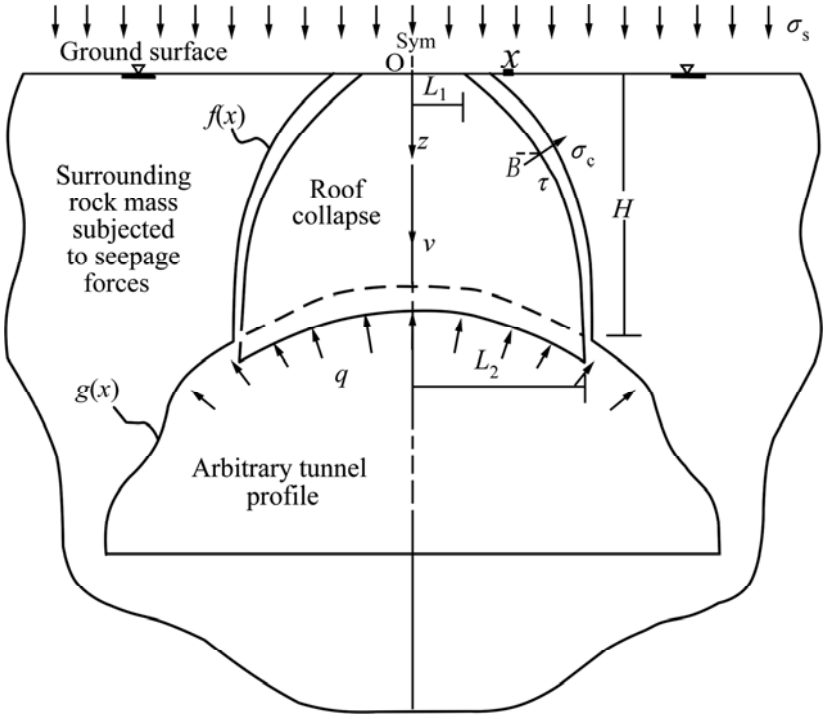

Fig. 1 Collapsing block on condition of seepage forces

3 Upper analysis with Hoek-Brown criterion under seepage

3.1 Hoek-Brown failure criterion

Hoek-Brown failure criterion is widely used for describing nonlinear characteristics of rock mass and it has two forms of expression which are represented by virtue of major and minor principal stresses and normal and shear stresses, respectively [28]. As the energy dissipation is created by normal and shear stresses, thus it is so convenient to use the latter form, it is

$$\tau = \mathrm{A}\sigma_{\mathrm{c}}[(\sigma_{\mathrm{n}} + \sigma_{\mathrm{t}})\sigma_{\mathrm{c}}^{-1}]^{B} \tag{1}$$

where σ_{n} and τ are the normal and shear stress, respectively, A and B are physical parameters of the rock; σ_{c} and σ_{t} represent the uniaxial compressive strength and the tensile strength of the rock mass, respectively.

3.2 Upper bound theorem

According to upper bound theorem, the actual collapsing load is no more than the load obtained by equating the rate of the energy dissipation to the external rate of work in any kinematically admissible velocity field when the velocity boundary condition is satisfied [32]. When the effect of seepage forces is taken into consideration in the realm of the upper bound theorem of limit analysis, the work of seepage forces is equal to the sum of seepage forces regarded as external loading working on skeleton expansion with referring to the previous work. Therefore, the effect of seepage forces incorporated to the upper bound theorem can be written as

$$\int_{\Omega} \sigma_{ij}\dot{\varepsilon}_{ij}\,\mathrm{d}\Omega \geq \int_{s} T_i v_i\,\mathrm{d}s + \int_{\Omega} X_i v_i\,\mathrm{d}\Omega + \int_{\Omega} -\mathrm{grad}u\, v_i\,\mathrm{d}\Omega - \int_{s} \boldsymbol{n}_i u v_i\,\mathrm{d}S \tag{2}$$

where σ_{ij} and $\dot{\varepsilon}_{ij}$ represent the stress tensor and strain rate in the kinematically admissible velocity field separately, respectively; T_i is a surface load on boundary s; X is the body force, Ω is the volume of the collapsing block; v_i is the velocity along the velocity discontinuity surface; u is the pore pressure; $\boldsymbol{n}_i$ is the unit normal vector at the directed surface S; −grad u is excess pore pressure. When using the expression above to analyze the stability of geotechnical engineering, the material should be perfectly plastic and follows an associated flow rule.

4 Limit analysis and variational method

4.1 Energy dissipation and external rate of work in circular tunnel

When the roof of tunnels tends to slide under the limit state on the detaching surface, the energy dissipation of a random point on the velocity discontinuity surface created by shear and normal stresses can be obtained as Eq. (9) in Ref. [22]. The total energy dissipation rate caused by the internal forces on the detaching surface through integrating D_i over the

interval $[L_1, L_2]$ is

$$D=\int_s D_i t\mathrm{d}S= 2\pi\int_{L1}^{L_2}[\sigma_t-\sigma_c(AB)^{1/(1-B)}(1-B^{-1})f'(x)^{1/(1-B)}]xv\,\mathrm{d}x \tag{3}$$

where $f'(x)$ is the first derivative of $f(x)$, t is the thickness of the detaching surface, and dS is the infinitesimal lateral area on the detaching surface, which can be calculated as

$$\mathrm{d}S=2\pi x\sqrt{1+f'(x)^2}\,\mathrm{d}x \tag{4}$$

Considering that the collapsing block is derived with three-dimensional rotational mechanism, the work rate of failure block caused by weight can be expressed as

$$P_{\gamma'}=\gamma'\int_{L_1}^{L_2}\pi x^2 f'(x)v\mathrm{d}x-\gamma'\int_0^{L_2}\pi x^2 g'(x)v\mathrm{d}x \tag{5}$$

where γ' is the buoyant weight which can be computed by $\gamma'=\gamma-\gamma_w$, L_1 and L_2 are the widths of the collapse block shown in Fig. 1. The work rate of supporting pressure in shallow circular tunnel is

$$P_q=\int_0^{\arcsin\frac{L_2}{R}}2\pi qR^2 v\sin\theta\cos\theta\mathrm{d}\theta\cos\pi=\pi L_2^2 qv\cos\pi \tag{6}$$

where q is the supporting pressure exerted on the lining of tunnel, R is the radius of the circular tunnel. As the effect of surcharge on the roof collapse is not neglected, the power of ground surcharge is

$$P_s=\pi L_1^2\sigma_s v \tag{7}$$

where σ_s is the surcharge load acting on the ground surface. With referring to the work of SAADA et al [31], the distribution of excess pore pressure is defined as

$$u=p-p_w=p-\gamma_w h \tag{8}$$

where p is the pore water pressure at the considered point which can be calculated as $p=r_p\gamma h$, r_p represents pore pressure coefficient, and $p_w=\gamma_w h$, is the hydrostatic distribution for pore pressure, γ_w referring to the water unit weight, h is the vertical distance between the point in collapsing block and the ground.

Then, −grad u can be calculated by

$$-\mathrm{grad}\,u=-\mathrm{d}u/\mathrm{d}h=\gamma_w-r_p\gamma \tag{9}$$

Consequently, the work rate produced by seepage forces in the body of roof collapse is

$$P_{u\Omega}=\int_\Omega-\mathrm{grad}\,u\,v\,\mathrm{d}\Omega= \int_{L1}^{L_2}(\gamma_w-r_p\gamma)\pi x^2 f'(x)v\,\mathrm{d}x- \int_0^{L_2}(\gamma_w-r_p\gamma)\pi x^2 g'(x)v\,\mathrm{d}x \tag{10}$$

and the work of water pressure, including seepage forces and hydrostatic pressure, along the velocity discontinuity surface is

$$P_{uS}=-\int_s u'\boldsymbol{n}_i v_i\,\mathrm{d}S= -\int_{L1}^{L_2}u'2\pi xv\mathrm{d}x\cos\pi=\int_{L1}^{L_2}2\pi x r_p\gamma f(x)v\mathrm{d}x \tag{11}$$

where the water pressure along the detaching surface is calculated by virtue of $u'=(r_p\gamma-\gamma_w)f(x)+\gamma_w f(x)=r_p\gamma f(x)$. Consequently, an objective function which is comprised of the internal energy rate of dissipation and the external rate of work can be set up as

$$\begin{aligned}\zeta&=D-P_{\gamma'}-P_q-P_s-P_{u\Omega}-P_{uS}=\\&2\pi\int_{L1}^{L_2}\left\{\left[\sigma_t-\sigma_c(AB)^{1/(1-B)}(1-B^{-1})f'(x)^{1/(1-B)}\right]x-\frac{1-r_p}{2}\gamma x^2 f'(x)-r_p\gamma f(x)x\right\}\cdot\\&\mathrm{d}x+\int_0^{L_2}(1-r_p)\gamma\pi x^2 g'(x)v\mathrm{d}x+\pi L_2^2 qv-\pi L_1^2\sigma_s v=\\&2\pi\int_{L1}^{L_2}\psi v\mathrm{d}x+\int_0^{L_2}(1-r_p)\gamma\pi x^2 g'(x)v\mathrm{d}x+\\&\pi L_2^2 qv-\pi L_1^2\sigma_s v\end{aligned} \tag{12}$$

where $\psi[f(x), f'(x), x]$ is a function expressed as

$$\psi[f(x),f'(x),x]= \left[\sigma_t-\sigma_c(AB)^{1/(1-B)}(1-B^{-1})f'(x)^{1/(1-B)}\right]x- \frac{1-r_p}{2}\gamma x^2 f'(x)-r_p\gamma f(x)x \tag{13}$$

According to upper bound theorem, for the purpose of making the integral ψ over the interval $[L_1, L_2]$ achieve an extreme value, it is a classical problem of the calculus of variations, i.e., to find a function, $y=f(x)$, which makes Eq. (13) reach a stationary value under the condition of customary regularity. Then, the expression of ψ is a function which can be turned into an Euler's equation, which can be expressed as

$$\delta\psi[f(x),f'(x),x]=0\ \Rightarrow\ \frac{\partial\psi}{\partial f(x)}-\frac{\partial}{\partial x}\left[\frac{\partial\psi}{\partial f'(x)}\right]=0 \tag{14}$$

According to Eq. (13), the Euler equation of this problem is obtained

$$\sigma_c(AB)^{1/(1-B)}\left[(1-B)^{-1}f'(x)^{(2B-1)/(1-B)}f''(x)x+ B^{-1}f'(x)^{B/(1-B)}\right]-(1-2r_p)\gamma x=0 \tag{15}$$

By introducing a coefficient m, that is

$$m=(1-B)^{-1}\sigma_c(AB)^{1/(1-B)} \tag{16}$$

Equation (15) can be rewritten as follows in a succinct form.

$$mf'(x)^{(2B-1)/(1-B)}f''(x)x+B^{-1}(1-B)mf'(x)^{B/(1-B)}-(1-2r_p)\gamma x=0 \tag{17}$$

Obviously, Eq. (17) is a nonlinear second-order differential equation which can be coped with degree reduction, i.e. $f'(x)=w$, then, $f''(x)=\mathrm{d}w/\mathrm{d}x$, therefore, Eq. (17) is worked out as

$$\frac{\mathrm{d}w}{\mathrm{d}x}=\frac{B-1}{B}\frac{w}{x}+\frac{(1-2r_\mathrm{p})\gamma}{m}w^{\frac{1-2B}{1-B}} \tag{18}$$

The expression above is a Bernoulli equation, thus supposing $t=w^{B/(1-B)}$, so as to make some algebraic operations, it can be converted into a linear first-order differential equation, that is

$$\frac{\mathrm{d}t}{\mathrm{d}x}+\frac{t}{x}=\frac{(1-2r_\mathrm{p})\gamma}{m}\frac{B}{1-B} \tag{19}$$

According to corresponding integral formula, the expression of t can be calculated as

$$t=\frac{(1-2r_\mathrm{p})\gamma}{2m}\frac{B}{1-B}x+\frac{c}{x} \tag{20}$$

where c is a constant to be determined. Meanwhile, considering $t=w^{B/(1-B)}=f'(x)^{B/(1-B)}$, the representation of $f'(x)$ is

$$f'(x)=\left[\frac{(1-2r_\mathrm{p})\gamma}{2m}\frac{B}{1-B}x+\frac{c}{x}\right]^{(1-B)/B} \tag{21}$$

Based on mechanical analysis, there exists an implicit condition that the shear component of stress disappears on the coordinate points of ($x=L_1$, $z=0$), it results

$$c=-\frac{(1-2r_\mathrm{p})\gamma}{2m}\frac{B}{1-B}L_1^2 \tag{22}$$

Thus, the explicit form of $f'(x)$ can be obtained as

$$f'(x)=\left[\frac{(1-2r_\mathrm{p})\gamma}{2m}\frac{B}{1-B}\left(x-\frac{L_1^2}{x}\right)\right]^{(1-B)/B}=A^{-1/B}B^{-1}\left[\frac{(1-2r_\mathrm{p})\gamma}{2\sigma_\mathrm{c}}\right]^{(1-B)/B}\left(x-\frac{L_1^2}{x}\right)^{(1-B)/B} \tag{23}$$

Indeed, the expression of $f'(x)$ is a complicated hyperbolic function and can be rewritten as

$$f'(x)=A^{-1/B}B^{-1}\left[\frac{(1-2r_\mathrm{p})\gamma}{2\sigma_\mathrm{c}}\right]^{(1-B)/B}\cdot\left(\frac{x+L_1}{x}\right)^{(1-B)/B}(x-L_1)^{(1-B)/B} \tag{24}$$

Considering the analytical solution of $f(x)$ by integrating $f'(x)$ over the interval $[L_1, L_2]$ is difficult to derive, it makes sense by making a little simplification. Due to $L_1\le x\le L_2$, obviously, it can lead to $\frac{L_2+L_1}{L_2}\le\frac{x+L_1}{x}\le 2$. Consequently, choosing the medium value is a simplified way to make further calculation, that is $\frac{x+L_1}{x}\approx\frac{L_1+3L_2}{2L_2}$. The influence on the results illustrated in the latter is rather small and so the explicit expression of $f(x)$ is obtained by virtue of integration.

$$f(x)=A^{-1/B}\left[\frac{(1-2r_\mathrm{p})\gamma}{2\sigma_\mathrm{c}}\left(\frac{L_1+3L_2}{2L_2}\right)\right]^{(1-B)/B}\cdot(x-L_1)^{1/B}-h_0 \tag{25}$$

where h_0 is an integration constant decided by $f(x=L_1)=0$, and it leads to $h_0=0$. There is another geometric equation to be satisfied, as illustrated in Fig. 1.

$$f(x=L_2)=g(x=L_2)=H \tag{26}$$

As a consequence,

$$H=A^{-1/B}\left[\frac{(1-2r_\mathrm{p})\gamma}{2\sigma_\mathrm{c}}\left(\frac{L_1+3L_2}{2L_2}\right)\right]^{(1-B)/B}(L_2-L_1)^{1/B} \tag{27}$$

Therefore, the approximate form of detaching curve, $f(x)$, is derived after simplification in the plane. With the help of rotational failure mechanism, three-dimensional velocity discontinuity field is obtained:

$$f(x,y)=A^{-1/B}\left[\frac{(1-2r_\mathrm{p})\gamma}{2\sigma_\mathrm{c}}\left(\frac{L_1+3L_2}{2L_2}\right)\right]^{(1-B)/B}\cdot\left(\sqrt{x^2+y^2}-L_1\right)^{1/B} \tag{28}$$

Owing to the cross section of tunnel is circular, then the form of $g(x)$ can be expressed as below according to geometrical condition,

$$g(x)=H+\sqrt{R^2-L_2^2}-\sqrt{R^2-x^2} \tag{29}$$

Then, it is

$$g'(x)=x/\sqrt{R^2-x^2} \tag{30}$$

By substituting Eq. (25) into Eq. (13), ψ is derived.

$$\psi=\sigma_\mathrm{t}x-D\left(1-\frac{1}{B}\frac{L_1+L_2}{L_1+3L_2}\right)(x-L_1)^{\frac{1+B}{B}}-DL_1\left(1+\frac{1}{B}\frac{L_2-L_1}{L_1+3L_2}\right)(x-L_1)^{\frac{1}{B}}-\frac{D}{B}\frac{2L_1^2L_2}{L_1+3L_2}(x-L_1)^{\frac{1-B}{B}} \tag{31}$$

where

$$D=A^{-1/B}\sigma_\mathrm{c}^{(B-1)/B}\left[\frac{(1-2r_\mathrm{p})\gamma}{2}\left(\frac{L_1+3L_2}{2L_2}\right)\right]^{1/B} \tag{32}$$

By virtue of calculating the integral of ψ over the

interval $[L_1, L_2]$ according to Eq. (12), the form of ζ in circular tunnel is computed as

$$\zeta = 2\pi\int_{L1}^{L_2}\psi[f(x), f'(x), x]v\mathrm{d}x + \int_0^{L_2}\left(1-r_\mathrm{p}\right)\gamma\pi x^2 g'(x)v\mathrm{d}x + \pi L_2^2 qv - \pi L_1^2\sigma_s v = \pi\sigma_t\left(L_2^2 - L_1^2\right)v - D\left(1-\frac{1}{B}\frac{L_1+L_2}{L_1+3L_2}\right)\cdot\frac{2\pi B}{1+2B}\left(L_2-L_1\right)^{\frac{1+2B}{B}}v - D\frac{4\pi L_1^2 L_2}{L_1+3L_2}\left(L_2-L_1\right)^{1/B}v + \pi L_2^2 qv - DL_1\left(1+\frac{1}{B}\frac{L_2-L_1}{L_1+3L_2}\right)\frac{2\pi B}{1+B}\left(L_2-L_1\right)^{\frac{1+B}{B}}v + \left(1-r_p\right)\gamma\pi\left[\frac{2}{3}R^3 - \sqrt{R^2-L_2^2}\left(\frac{2}{3}R^2+\frac{1}{3}L_2^2\right)\right]v - \pi L_1^2\sigma_s v \tag{33}$$

At last, on the basis of upper bound theorem of limit analysis, it can be computed by equating the external rate of work to the rate of the energy dissipation, i.e.,

$$\sigma_\mathrm{t}(L_2^2-L_1^2) - D\left(1-\frac{1}{B}\frac{L_1+L_2}{L_1+3L_2}\right)\frac{2B}{1+2B}(L_2-L_1)^{\frac{1+2B}{B}} - D\frac{4L_1^2L_2}{L_1+3L_2}(L_2-L_1)^{\frac{1}{B}} + L_2^2 q - L_1^2\sigma_s - DL_1\left(1+\frac{1}{B}\frac{L_2-L_1}{L_1+3L_2}\right)\frac{2B}{1+B}(L_2-L_1)^{\frac{1+B}{B}} + (1-r_\mathrm{p})\gamma\left[\frac{2}{3}R^3 - \sqrt{R^2-L_2^2}\left(\frac{2}{3}R^2+\frac{1}{3}L_2^2\right)\right] = 0 \tag{34}$$

As the expression of $f(x)$ is derived, then the volume of roof collapse in circular tunnel can be calculated as

$$V = \int_{L_1}^{L_2}\pi x^2 f'(x)\mathrm{d}x - \int_0^{L_2}\pi x^2 g'(x)\mathrm{d}x = \pi A^{-1/B}B^{-1}\left[\frac{(1-2r_\mathrm{p})\gamma}{2\sigma_\mathrm{c}}\left(\frac{L_1+3L_2}{2L_2}\right)\right]^{(1-B)/B}\cdot\left[\frac{B}{1+2B}\left(L_2-L_1\right)^{\frac{1+2B}{B}} + \frac{2BL_1}{1+B}\left(L_2-L_1\right)^{\frac{1+B}{B}} + BL_1^2\cdot\left(L_2-L_1\right)^{\frac{1}{B}} - \right] - \pi\left[\frac{2}{3}R^3 - \sqrt{R^2-L_2^2}\left(\frac{2}{3}R^2+\frac{1}{3}L_2^2\right)\right] \tag{35}$$

4.2 Energy dissipation and external rate of work in square tunnel

In a similar way, the rate of energy dissipation and external rate of work in square tunnel can be obtained. In comparison with the calculation of that in circular tunnel, the power of supporting pressure in shallow rectangular tunnel is

$$P_\mathrm{q} = \pi L_2^2 qv\cos\pi \tag{36}$$

from which it can be immediately noticed that it has the same expression with that in circle tunnel, thus the expression of $f(x, y)$ remains the same form with Eq. (28) in rectangular tunnel for other calculation is perfectly identical. Considering the geometric condition of square tunnel, the profile is the horizontal and so $g(x)=H$, $g'(x)=0$. Consequently, the expression of ζ in square tunnel is

$$\zeta = 2\pi\int_{L1}^{L_2}\psi[f(x), f'(x), x]v\mathrm{d}x + \int_0^{L_2}\left(1-r_\mathrm{p}\right)\gamma\pi x^2 g'(x)v\mathrm{d}x + \pi L_2^2 qv - \pi L_1^2\sigma_\mathrm{s} v = \pi\sigma_\mathrm{t}\left(L_2^2-L_1^2\right)v - D\left(1-\frac{1}{B}\frac{L_1+L_2}{L_1+3L_2}\right)\frac{2\pi B}{1+2B}\cdot\left(L_2-L_1\right)^{\frac{1+2B}{B}}v + \pi L_2^2 qv - \pi L_1^2\sigma_\mathrm{s} v - DL_1\left(1+\frac{1}{B}\frac{L_2-L_1}{L_1+3L_2}\right)\frac{2\pi B}{1+B}\left(L_2-L_1\right)^{\frac{1+B}{B}}v - D\frac{4\pi L_1^2L_2}{L_1+3L_2}\left(L_2-L_1\right)^{1/B}v \tag{37}$$

and then by equating the external rate of work to the rate of the energy dissipation, that is

$$\sigma_\mathrm{t}\left(L_2^2-L_1^2\right) - D\left(1-\frac{1}{B}\frac{L_1+L_2}{L_1+3L_2}\right)\frac{2B}{1+2B}\cdot\left(L_2-L_1\right)^{(1+2B)/B} + L_2^2 q - L_1^2\sigma_\mathrm{s} - DL_1\left(1+\frac{1}{B}\frac{L_2-L_1}{L_1+3L_2}\right)\frac{2B}{1+B}\left(L_2-L_1\right)^{(1+B)/B} - D\frac{4L_1^2L_2}{L_1+3L_2}\left(L_2-L_1\right)^{1/B} = 0 \tag{38}$$

By virtue of combining Eq. (27) with Eq. (38), the collapse widths, L_1 and L_2, can be worked out. As a consequence, the volume of collapsing block in square tunnel can be expressed as

$$V = \int_{L_1}^{L_2}\pi x^2 f'(x)\mathrm{d}x - \int_0^{L_2}\pi x^2 g'(x)\mathrm{d}x = \pi A^{-1/B}B^{-1}\left[\frac{(1-2r_\mathrm{p})\gamma}{2\sigma_\mathrm{c}}\left(\frac{L_1+3L_2}{2L_2}\right)\right]^{(1-B)/B}\cdot\left[\frac{B}{1+B}(L_2-L_1)^{(1+2B)/B} + \frac{2BL_1}{1+B}(L_2-L_1)^{(1+B)/B} + BL_1^2(L_2-L_1)^{1/B}\right] \tag{39}$$

5 Numerical results and discussion

5.1 Comparison with previous work

By virtue of upper bound theorem and variational

approach, the solution of describing the shape of velocity discontinuity surface is obtained. In order to verify the validity and agreement of the method proposed, corresponding comparison with the previous work should be conducted. For a circular tunnel, YANG and HUANG [20] derived the numerical solutions of the collapsing width in shallow tunnel without taking seepages forces and surface load into account, so the value of pore pressure coefficient r_p and σ_s should be set to zero when comparing with their work. Table 1 shows the numerical results of the parameters corresponding to B=3/4, A=0.1, σ_c=2.5 MPa, σ_t=σ_c/100, R=5 m, γ= 25 kN/m^3, q=100 kPa, r_p=0, σ_s=0, H=8 m were worked out in comparison with the work of YANG and HUANG [20].

Table 1 Comparison of existing and present solutions in shallow circular tunnel

Solutions	Ref. [20]	This work	Difference
L_1/m	2.870 5	2.472 4	13.9%
L_2/m	4.931 9	4.383 9	11.1%

It can be found that the widths of collapsing block, L_1 and L_2, calculated in this work when r_p=0 and σ_s=0 are approximately equal to those obtained by YANG and HUANG [20] from Table 1, in which the maximum difference is 13.9%. The results show that the solution derived in this work for charactering the failure mechanism of roof collapse has good agreement and validity in comparison with previous work.

5.2 Effects of different parameters on shape of roof collapse

In order to predict the impending roof collapse of tunnel with Hoek-Brown criterion, the numerical method has been employed to analyze the scope of collapsing block. Due to the fact that three-dimensional failure mechanism is derived from the plane collapse mechanism by rotating 360 °, every failure surface presents the same shape and also has identical properties, so it would be convenient to choose a plane to discuss the impact of parameters on collapsing scope. For a square tunnel, the numerical results are calculated using Eq. (27) and Eq. (38). Consequently, different shapes of roof collapse in two dimensions can be plotted in Fig. 2. Moreover, the numerical results of width as well as the volume of collapsing block in rectangular tunnel are given in Table 2.

It appears apparently in Fig. 2 that, along with the increasing values of σ_c and r_p, the dimensions of the roof collapse have a trend to increase. While with the increase of B and γ, the widths, L_1 and L_2, of the collapsing block tend to decrease. It can be immediately found that the

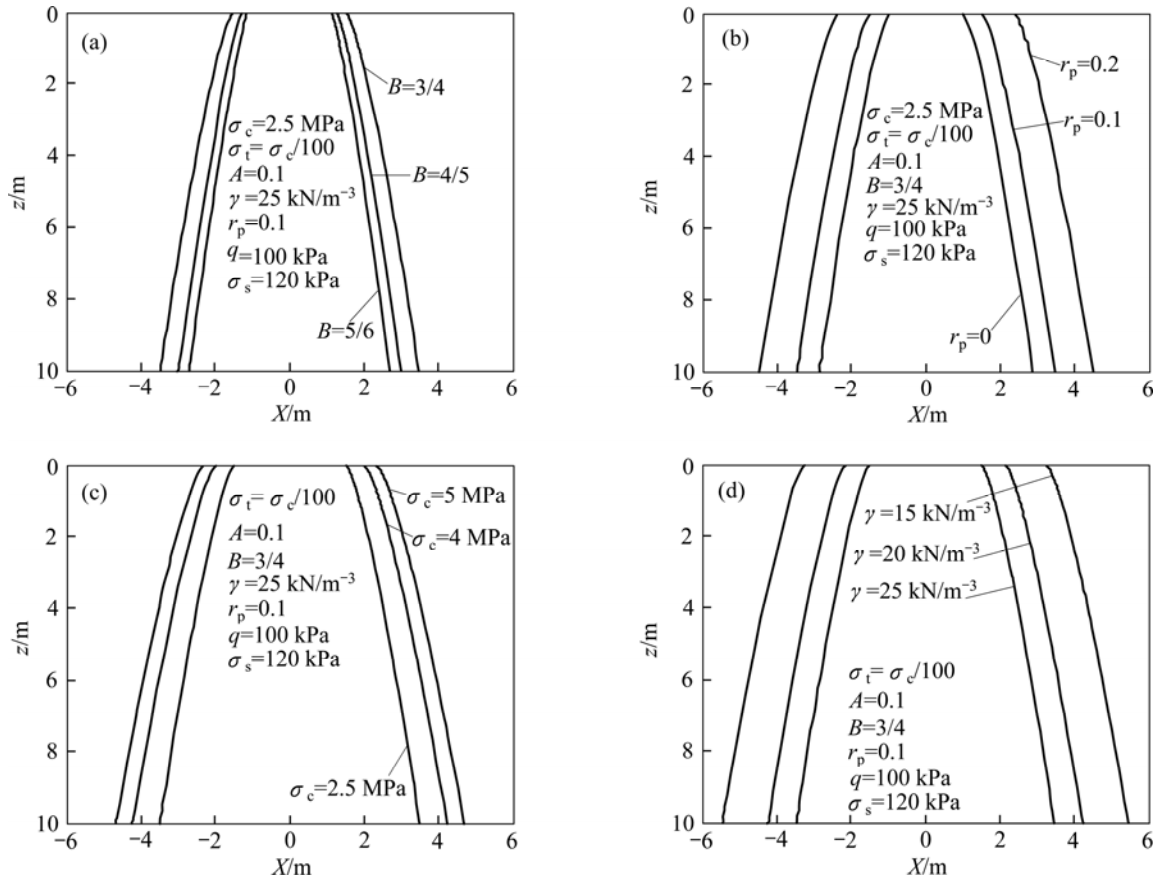

Fig. 2 Shape of roof collapse in shallow square tunnel with respect to different parameters: (a) B; (b) r_p; (c) σ_c; (d) γ

Table 2 Collapsing dimensions in shallow square tunnel under different parameters

B	σ_c/MPa	σ_t/MPa	γ/(kN·m^{-3})	r_p	L_1/m	L_2/m	V/m^3
3/4	2.5	0.025	25	0.2	1.527 2	3.479 9	228.257 7
4/5	2.5	0.025	25	0.2	1.282 5	2.991 6	163.480 1
5/6	2.5	0.025	25	0.2	1.141 9	2.705 5	157.427 3
3/4	2.5	0.025	25	0.2	1.527 2	3.479 9	228.257 7
3/4	4.0	0.040	25	0.2	2.026 3	4.215 9	348.543 3
3/4	5.0	0.050	25	0.2	2.358 0	4.669 2	437.485 6
3/4	2.5	0.025	25	0.2	1.527 2	3.479 9	228.257 7
3/4	2.5	0.025	20	0.2	2.181 4	4.234 8	363.289 3
3/4	2.5	0.025	15	0.2	3.283 6	5.477 2	657.834 9
3/4	2.5	0.025	25	0	1.012 0	2.870 6	143.121 8
3/4	2.5	0.025	25	0.1	1.527 2	3.479 9	228.257 7
3/4	2.5	0.025	25	0.2	2.401 0	4.484 9	415.331 0

volume of roof collapse presents the same law with its collapsing dimensions in Table 2. The change rule of σ_c, B and γ is in complete accord with the research of FRALDI and GUARRACINO [21−22], that is, it shows great validity by comparing with the former work. Obviously, the seepage forces acting on the underground structures have a significant influence on the dimensions of roof collapse, which has also been illustrated in Fig. 2.

5.3 Effects of hypothetic curve $f'(x)$ on collapsing blocks

The implicit solution of $f(x)$ derived is based on the assumption, which means that it is just an approximate result. By virtue of making the graph of $f'(x)$ shown in Fig. 3, in which the parameters are characterized by A=0.1, B=3/4, γ=25 kN/m^3, σ_c=2.5 MPa, σ_t=σ_c/100, r_p= 0.1, p=100 kPa and σ_s=120 kPa, it is noticed that the difference between the hypothetic curve and the actual curve of $f'(x)$ is relatively small, which indicates that replacing the actual curve of $f'(x)$ with the hypothetic curve is valid.

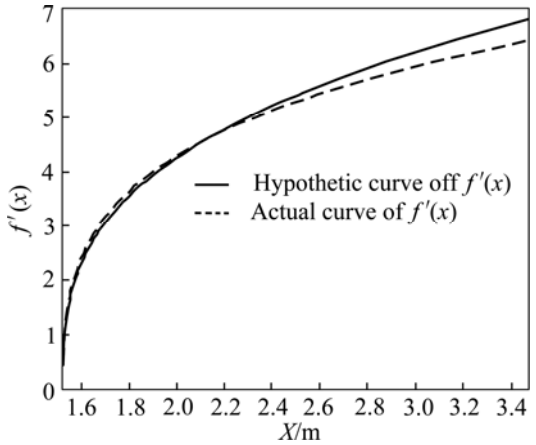

Fig. 3 Comparison of results between hypothetic curve and actual curve of $f'(x)$

6 Conclusions

1) By constructing a three-dimensional rotational collapse mechanism under the condition of seepage forces, the approximate solution of velocity discontinuity surface in three dimensions is derived with the help of upper bound theorem and the tool of calculus of variations according to Hoek-Brown failure criterion. The effect of seepage forces is regarded as a work rate of external force incorporated to upper bound theorem and it has a detrimental impact on the stability of tunnel to a large degree. The parametric study indicates that the bottom and the top widths of the collapsing block tend to decrease along with the decrease of σ_c and r_p, but increase with the decrease of B and γ.

2) Based on the work in the stability analysis of rock slopes subjected to seepage forces with limit analysis method, the corresponding idea is used to derive the shape of impending collapsing block with three dimensions in square or circular tunnel and the solution shows great validity by comparing with the previous work. The method proposed in this work to predicate the roof collapse can be taken as a complementary tool and reference to stability analysis of tunnel.

References

[1] KIM J, SALGADO R, YU H S. Limit analysis of slopes subjected to pore-water pressures [J]. Journal of Geotechnical and Geoenvironmental Engineering, 1999, 125(1): 49−58.

[2] MICHALOWSKI R L. Stability charts for uniform slopes [J]. Journal of Geotechnical and Geoenvironmental Engineering, 2002, 128(4): 351−355.

[3] SOUBRA A H. Static and seismic passive earth pressure coefficients on rigid retaining structure [J]. Canadian Geotechnical Journal, 2000, 37(2): 463−478.

[4] AGAR J G, MORGENSTERN N R, SCOTT J. Shear strength and stress-strain behavior of Athabasca oil sand at elevated temperatures and pressure [J]. Canadian Geotechnical Journal, 1985, 24(1): 1−10.

[5] BAKER R. Nonlinear Mohr envelopes based on triaxial data [J]. Journal of Geotechnical and Geoenvironmental Engineering, 2004, 130(5): 498−506.

[6] YANG X L, LI L, YIN J H. Seismic and static stability analysis for rock slopes by a kinematical approach [J]. Geotechnique, 2004, 54(8): 543−549.

[7] YANG X L, YIN J H. Slope stability analysis with nonlinear failure criterion [J]. Journal of Engineering Mechanics, 2004, 130(3): 267−273.

[8] YANG X L, YIN J H. Upper bound solution for ultimate bearing capacity with a modified Hoek-Brown failure criterion [J]. International Journal of Rock Mechanics and Mining Sciences, 2005, 42(4): 550−560.

[9] YANG X L, YIN J H. Estimation of seismic passive earth pressures with nonlinear failure criterion [J]. Engineering Structures, 2006, 28(3): 342−348.

[10] LAM L, FREDLUND D G. A general limit equilibrium model for three-dimensional slope stability analysis [J]. Canadian Geotechnical Journal, 1993, 30(6): 905−919.

[11] CHEN Z Y, WANG X G, HABERFIEDL C. A three-dimensional slope stability analysis method using the upper bound theorem [J]. International Journal of Rock Mechanics and Mining Sciences, 2001, 38(1): 69−378.

[12] DONALD I B, CHEN Z Y. Slope stability analysis by the upper bound approach: Fundamentals and methods [J]. Canadian Geotechnical Journal, 1997, 34(6): 853−862.

[13] ANAGNOSTOU G, KOVÁRI K. Face stability conditions with earth-presssure-balanced shields [J]. Tunnelling and Underground Space Technology, 1996, 11(2): 165−173.

[14] LECA E, DORMIEUX L. Upper and lower solutions for the space stability of shallow circular tunnels in frictional material [J]. Geotechnique, 1990, 40(4): 581−606.

[15] SOUBRA A H, DIAS D, EMERIAULT F. Three-dimensional face stability analysis of circular tunnels by a kinematical approach [C]// Proceedings of the Geocongress Characterization Monitoring and Modelling of Geosystems, New Orleans, 2008: 9−12.

[16] CHAMBON P, CORTÉ J F. Shallow tunnels in cohesionless soil: Stability of tunnel face [J]. Journal of Geotechnical Engineering, 1994, 120(7): 1148−1165.

[17] YANG X L, ZHANG J H, JIN Q Y, MA J Q. Analytical solution to rock pressure acting on three shallow tunnels subjected to unsymmetrical loads [J]. Journal of Central South University, 2013, 20(2): 528−535.

[18] YANG X L, JIN Q Y, MA J Q. Pressure from surrounding rock of three shallow tunnels with large section and small spacing [J]. Journal of Central South University, 2012, 19(8): 2380−2385.

[19] YANG X L, HUANG F. Three-dimensional failure mechanism of a rectangular cavity in a Hoek–Brown rock medium [J]. International Journal of Rock Mechanics and Mining Sciences, 2013, 61: 189−195.

[20] YANG X L, HUANG F. Collapse mechanism of shallow tunnel based on nonlinear Hoek-Brown failure criterion [J]. Tunnelling and Underground Space Technology, 2011, 26(6): 686−691.

[21] MOLLON G, DIAS D, SOUBRA A H. Rotational failure mechanisms for the face stability analysis of tunnels driven by a pressurized shield [J]. International Journal for Numerical and Analytical Methods in Geomechanics, 2011, 25(12): 1363−1388.

[22] FRALDI M, GUARRACINO F. Limit analysis of collapse mechanisms in cavities and tunnels according to the Hoek–Brown failure criterion [J]. International Journal of Rock Mechanics and Mining Sciences, 2009, 46(4): 665−673.

[23] FRALDI M, GUARRACINO F. Analytical solutions for collapse mechanisms in tunnels with arbitrary cross sections [J]. International Journal of Solids and Structures, 2010, 47(2): 216−223.

[24] YANG X L, ZOU J F. Cavity expansion analysis with non-linear failure criterion [J]. Proceedings of the Institution of Civil Engineers-Geotechnical Engineering, 2011, 164(1): 41−49.

[25] YANG X L. Seismic passive pressures of earth structures by nonlinear optimization [J]. Archive of Applied Mechanics, 2011, 81(9): 1195−1202.

[26] YANG X L, WANG J M. Ground movement prediction for tunnels using simplified procedure [J]. Tunnelling and Underground Space Technology, 2011, 26(3): 462−471.

[27] LEE I M, NAM S W. The study of seepage forces acting on the tunnel lining and tunnel face in shallow tunnels [J]. Tunnelling and Underground Space Technology, 2001, 16(1): 31−40.

[28] HOEK E, BROWN E T. Practical estimate the rock mass strength [J]. International Journal of Rock Mechanics and Mining Sciences, 1997, 34(8): 1165−1186.

[29] YANG X L. Seismic bearing capacity of a strip footing on rock slopes [J]. Canadian Geotechnical Journal, 2009, 46(8): 943−954.

[30] YANG X L, YIN J H. Slope equivalent Mohr-Coulomb strength parameters for rock masses satisfying the Hoek-Brown criterion [J]. Rock Mechanics and Rock Engineering, 2010, 43(4): 505−511.

[31] SAADA Z, MAGHOUS S, GARNIER D. Stability analysis of rock slopes subjected to seepage forces using the modified Hoek–Brown criterion [J]. International Journal of Rock Mechanics and Mining Sciences, 2012, 55(1): 45−54.

[32] CHEN W F. Limit analysis and soil plasticity [M]. Amsterdam: Elsevier, 1975: 85−96.

(Edited by HE Yun-bin)